



Study on the Effects of Individual Pitot Tube Inlet of a Bladeless Tesla Microturbine using Numerical Analysis

Ernie Illyani Basri¹, Adi Azriff Basri^{1,*}, Farah Nur Diyana Salim¹

¹ Department of Aerospace Engineering, Faculty of Engineering, Universiti Putra Malaysia, 43400 UPM-Serdang, Selangor, Malaysia

ARTICLE INFO

Article history:

Received 2 June 2022

Received in revised form 5 July 2022

Accepted 7 August 2022

Available online 1 July 2023

Keywords:

Tesla turbine; Bladeless micro-turbine; Computational Fluid Dynamics; Multi-Reference Frame; Pitot Tube

ABSTRACT

In this paper, a comprehensive numerical analysis of a bladeless Tesla microturbine is presented. Various studies on the effects of Tesla design parameters have shown promising results. However, the limitations associated with the inherent nozzle design have often highlighted the low efficiency of the turbine. Therefore, the study was carried out using computational fluid dynamics (CFD) to demonstrate the efficiency of the turbine as a function of the performance of different openings of the inlet nozzles, i.e., as 1-opening and individual pitot tube opening. In this work, a validation study was performed with the existing manuscript before further investigating the effects of the different openings of the inlet nozzles. The results show that the configuration of 4 inlets with 4 openings (4i4o) results in higher velocity and pressure distribution compared to 4 inlets with 1 opening (4i1o). Consequently, 4i4o obtained a higher torque value compared to 4i1o with a difference of 10%. Hence, the thrust and efficiency values for the 4i4o were 33.69% and 34.30%, respectively, higher compared to the 4i1o. The performance of the Tesla turbine with the specified optimal configuration increased very significantly compared to the previous research studies. It can be concluded that the introduction of the functional theory of the 'pitot-tube', which considers the gaps individually by having a separate inlet for each of them, had a great impact on the performance of Tesla turbine.

1. Introduction

Renewable energies are sources of clean, inexhaustible and increasingly competitive energy. Compared to other growing consumption of primary fossil fuels and massive discharge of pollutants, hydroelectric power is one of the types of renewable energy, which the energy cleanly obtained from rivers or other freshwater currents that able to meet energy enlarging demand. Hence, energy shortfall and environmental destruction need to be taken into consideration. These consequences may significantly affect those rural areas, which demand energy electrification. And for these valid reasons, the awareness of using water turbine generator energy sources has captivated researchers around in recent years [1–6]. However, the available water turbine generator highlighted the disadvantage of the turbine blade may harm the ecology of aqua animals in the river. Due to its

* Corresponding author.

E-mail address: adiariff@upm.edu.my (Adi Azriff Basri)

features, Tesla bladeless turbine is an external generator system that is a powerful candidate for converting both potential and kinetic energies of the river to electrical power. The turbine consists of a set of stacked discs, as opposed to the blades in a conventional turbine. However, according to some research on Tesla bladeless turbine, the optimum efficiency obtained is only about 30-40%. Therefore, this research is conducted to increase the performance of energy efficiency in the bladeless Tesla turbine generator.

Tesla turbine is meant to replace the piston engine in generating power at that time in 1906. But it went sideways as the idea and technology itself were ahead of that particular time. Other than the turbine, the bladeless turbine can also be used as a pump or compressor which has been implemented in the medical field such as a blood transfusion pump [7]. In the first patent, Nikola Tesla introduced his basic bladeless design configuration as a pump or compressor. In the second patent, Tesla modified the basic compressor design and converted it to a turbine where the turbine was able to achieve 90% of efficiency, as Nikola Tesla claimed.

Tesla turbine consists of a shaft and multiple discs with a casing to contain the flow inside. It was meant to replace conventional turbines in generating power from these few components only. This is only possible to work based on the fundamental of fluid properties: adhesion and viscosity. Adhesion is the tendency of different molecules to stick to each other due to attractive forces. Cohesion is the tendency of similar molecules to stay together due to intermolecular attraction, as depicted in Figure 1. Other than that, viscosity also plays a vital role in rotating the disc. It is due to the resistance of a substance to flow, which in this case is air. When these two properties work together, they transfer energy from the fluid to the shaft, causing it to spin.

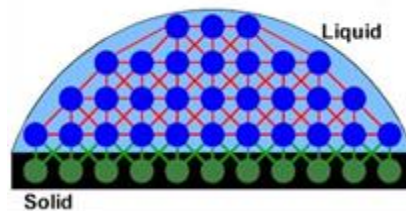


Fig. 1. Illustration of adhesion and cohesion of molecules

In specific, the breakdown of the process is as follows:

- i. As the flow passes through the disc, the adhesive force causes the fluid molecules just above the surface to stick onto the disc surface.
- ii. The molecules above those at the disc surface slowed down when they collided with the molecules sticking on the surface due to cohesive forces. These molecules slowed down the molecules above them.
- iii. As farther away from the disc surface, the fewer collision affected by the disc. This resulted in a thin film called a boundary layer that is forming over the surface.
- iv. At the same time, viscous forces cause the molecules to resist separation, which then generated the pulling forces to be transmitted to the disc. Therefore, the disc started to rotate following the flow direction.

Then propelling fluid accelerated rapidly in spiral behaviour along the disc surfaces until it reached the designated exit. As the fluid flows in the natural path of least resistance, it is free from the constraint and disruptive forces which may be caused by the vanes or blades, where it

experienced gradual changes in both velocity and direction. This means that more energy is transferred to the turbine which resulted in greater efficiency as the loss is small.

The power output of a bladeless turbine is determined by its mechanical power output or rotational speed. Centrifugal force is the driving factor for a disc to spin and create work. Referring to Figure 2, the centrifugal power is affected through the rotation of the rotor between the discs to provide its long spiral track. With the mechanical load off from the turbine, higher speed shows greater centrifugal power. Otherwise, the mechanical load grows leading to a drop in the speed, a low flow of centrifugal power, and a change in acceleration of the liquid track which turns more into the centre. This consequently enhances a bigger flow capacity through the mechanism.

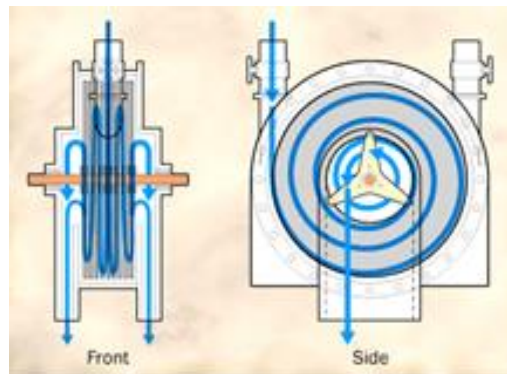


Fig. 2. Nikola Tesla turbine configuration

Even though the conventional turbines have been taking over the high power output niche as it has a great advantage over huge payload and high power density, the Tesla turbine is more efficient for the application of low output. It offers flexibility in the design option with low manufacturing cost, reduces vibration and hence improves safety. Although many investigations have been carried out in terms of experimental studies [8–22] and numerical/analytical studies [11, 14, 23–28], the result is still far from Tesla’s achievement. This is mostly due to the losses issue that needs to be accounted for designing and testing the turbine. Several parameters contributed to obtaining maximum efficiencies such as inlet and outlet geometry, arrangement of inlet and outlet, disc geometry and surface state, spacing between two discs and others.

In the year 1952, Armstrong [17] conducted an experimental study on the different nozzles; diverging nozzle and straight nozzle. The result showed that the diverging nozzle produced about one-third more horsepower than the straight nozzle for the case of the same pressure drop. In the numerical study by Jędrzejewski *et al.*, [26], the efficiency decreased directly as the number of nozzles and nozzle angle increased. In a further study, Sengupta *et al.*, [29] conducted a theoretical study on the inlet flow conditions of a three-dimensional (3D) fluid dynamics of the rotating flow. The results showed that the flow condition was within the casing, particularly the gap between casing and disk that contributed to obtaining optimum efficiency. Moreover, as the nozzle number increased leading to efficiency increased with decreasing the operable range speed, however, the non-axisymmetry condition decayed faster [30]. It can be concluded that the efficiency showed a significant reduction of more than four nozzles introduced [15, 31, 32]. In addition, the velocity losses at the inlet section might not be significant for a certain rotational speed, otherwise, this consequence might due to other factors [33].

Rice [24] pointed out that Tesla turbine nozzles are “necessarily long and inefficient”. Peshlakai *et al.*, [20] revealed that the slight changes in the nozzle geometry directly impacted the power produced by the turbine even though the rotor efficiency stayed relatively high. Recently, Sengupta [30] carried out a computational investigation regarding the nozzle effect through a various number

of nozzle inlets. However, for one type of design with the optimum number of nozzles, the efficiency obtained is only about 30-40%, which is still far beyond the claimed by Tesla with 90%. A recent study by Rusin *et al.*, [34] highlighted that the turbine efficiency has proven to surpass 20% by eliminating the impact of lateral gaps between the discs and the casing of a bladeless microturbine. In both studies of experimental and numerical, the result of efficiency was highly sensitive to the change in mass flow rate based on the efficiency of the individual gap to be around 14% to 24% and the lateral gaps of 1% to 4% between the rotor and the casing. Thus, overall turbine efficiency of almost 50% of total throughfighput flew through those gaps.

From the research study, the findings show that over the years, a lot of people have been investigating the performance of the Tesla turbine to achieve Tesla's expected efficiency of 90%. The trends of the studies and investigation are summarized in Figure 3.

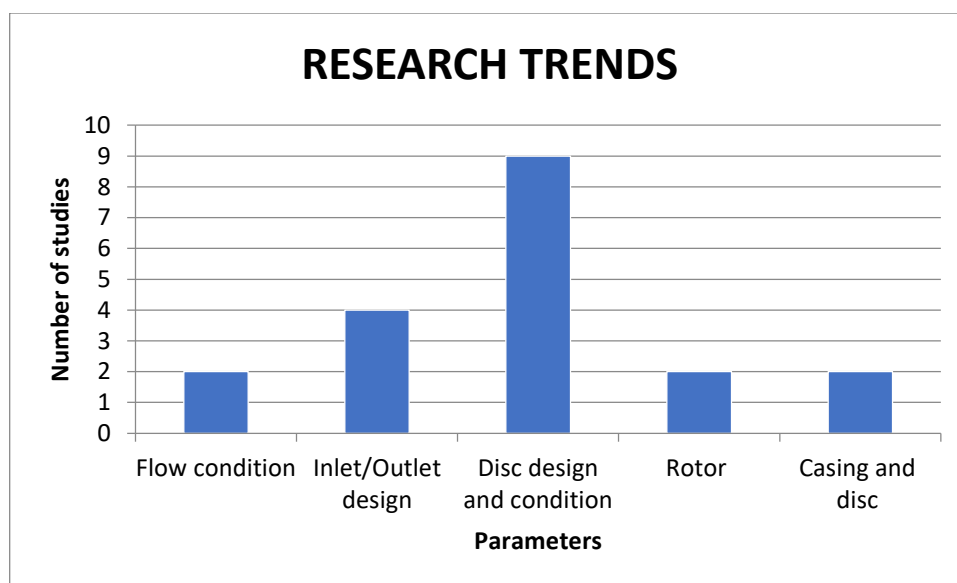


Fig. 3. Research trends on parameters investigated

Referring to Figure 3, it is noted that the important parameters in the Tesla turbine are investigated from 2008 to 2019. Those are flow condition of the fluid, inlet and outlet design of the turbine, disc design and condition or surface state, rotor size and geometry and clearance between casing and disc periphery or outer edge. From observation, most of the studies focused on the disc design and condition effects on the turbine performance, followed by inlet and outlet design and the other three parameters for equal times.

A major drawback of Tesla turbine design is the inlet loss. Fluid loses momentum as it experienced sudden expansion at the inlet-rotor junction. Although some research has been done on the effect of nozzles, the investigation was limited to one type of nozzle design, number as well as arrangement of nozzles around the casing. Every design has its limitation due to inconsistent manufacturing processes and internal losses contributed by the components. Therefore, a comparison of several designs of the nozzle is crucial. Furthermore, it is proven that the inlet nozzle plays a vital role in obtaining axis-symmetry conditions for the fluid flow in order to achieve maximum efficiency. Therefore, in this study, different types of inlet openings are investigated to determine the best performance of the Tesla turbine. Computational Fluid Dynamics (CFD) analysis with a multi-reference frame technique is applied throughout this study and the results of fluid flow behaviour in terms of velocity, pressure, torque, thrust, and power are compared in order to determine the best performance of Tesla turbine subjected to different inlet nozzle opening.

The paper is organized as follows: The first section presents the introduction of Tesla, and the second section highlights the methodology to conduct the numerical analysis. The results and discussions are in the third section and the final sections discuss the conclusion of the topic.

2. Methodology

2.1 Components Geometry and Dimensions

In this study, the design of a 3D model of the Tesla microturbine is prepared with the aid of the Computer-Aided Design (CAD) software of SolidWorks 2019. For the thin disc, the thickness is precisely 0.30 mm, with outer and inner diameters of 50.00 mm and 26.40 mm, respectively. Meanwhile, the casing has an outer and inner diameter of 50.40 mm and 26.4 mm with a thickness of 2.1 mm, respectively. The details specification of the important components such as the thin disc, casing or wall domain and its inlet, as in Table 1.



Table 1
 Components used for validation purposes

Components	Parameter	Dimensions (mm)
Thin disc	Outer diameter	50.0
	Inner diameter	26.4
	Thickness	0.3
Casing	Outer diameter	50.4
	Inner diameter	26.4
	Thickness	2.1
Inlet	Width	2.0
	Thickness	2.1

2.2 Inlet Design

In this study, two types of inlet openings which are 1-opening and 4-openings are introduced at the nozzle of the turbine design. The objective of introducing a 4-openings inlet nozzle is to direct the flow moving into the disc gaps individually in order to produce sufficient energy to rotate the disc and lead to higher torque. Table 2 shows the detailed view of the inlet with 1-opening and 4-openings. Meanwhile, Figures 4 and 5 show the Tesla micro-turbine of 4-inlets-1-opening (4i1o) and 4-inlets-4-openings (4i4o), respectively.

Table 2
 Specification of the inlet for further simulation

Inlet	1-opening	4-openings
Thin disc		
	Inlet with 1-opening	Inlet with 4-openings
Dimensions		
Width (mm)	2.0	2.0
Thickness (mm)	2.1	0.3 (each)

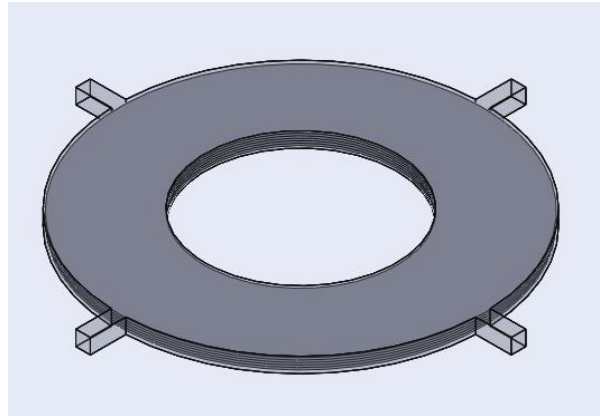


Fig. 4. Pitot of 4-inlets-1-opening (4i1o)

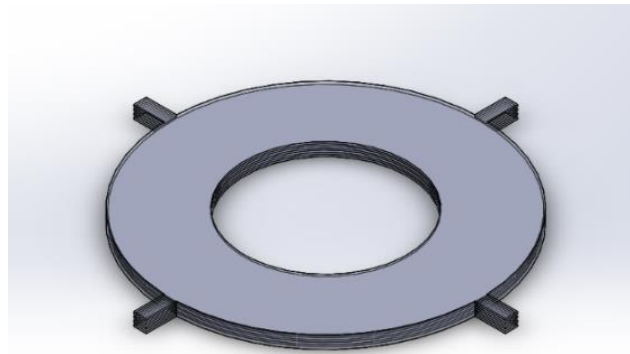


Fig. 5. Pitot of 4-inlets-4-opening (4i4o)

2.3 Computational Fluid Dynamics (CFD) Analysis

2.3.1 Theory of CFD

Computational Fluid Dynamics (CFD) is the simulation of fluid-based systems using modelling and numerical methods (discretization methods, solvers, numerical parameters, grid generations, etc). In order to solve the fluid flow problem, the physical properties of fluid must be known and then relevant mathematical equations which best described the physical properties are also included. For CFD, the governing equation used is Navier-Stokes. It is based on the conservation law of the physical properties of the fluid. The principle of conservational law is the change of properties, for example, mass, energy, and momentum, subjected to input and output.

For example, the change of mass in the object is as follows:

$$\frac{dM}{dt} = \dot{m}_{in} - \dot{m}_{out} = 0 \quad (1)$$

$$\dot{m}_{in} = \dot{m}_{out} \quad (2)$$

Navier-Stokes equation is obtained by applying the mass (continuity equation), momentum (momentum equation) and boundary conditions in terms of relative velocities; $U_r = V_r$; $U_z = V_z$; $U_\theta = (V_r + \Omega r)$. Based on a few assumptions in Ref. [35], the simplified conservation equations are as follows:

Continuity equation:

$$\frac{\partial V_r}{\partial r} + \frac{V_r}{r} = 0 \quad (3)$$

θ -Momentum equation:

$$V_r \frac{\partial V_\theta}{\partial r} + \frac{V_r V_\theta}{r} + 2\Omega V_r = \nu \frac{\partial^2 V_\theta}{\partial z^2} \quad (4)$$

r-Momentum equation:

$$V_r \frac{\partial V_r}{\partial r} - \Omega^2 r - 2\Omega V_\theta - \frac{V_\theta^2}{r} = -\frac{1}{\rho} \frac{dp}{dr} + \nu \frac{\partial^2 V_r}{\partial z^2} \quad (5)$$

z-Momentum equation:

$$\frac{\partial P}{\partial z} = 0 \quad (6)$$

Boundary condition:

$$\text{at } r = r_2 \quad \bar{V}_r = \bar{V}_{r2} \quad \bar{V}_\theta = \bar{V}_{\theta2} \quad (7)$$

$$\text{at } z = 0, b \quad \bar{V}_r = 0 \quad \bar{V}_\theta = 0 \quad (8)$$

$$\text{at } z = \frac{b}{2} \quad \frac{\partial V_r}{\partial z} = \frac{\partial V_\theta}{\partial z} = 0 \quad (9)$$

The schematic diagram for the mathematic solution is in Figure 6.

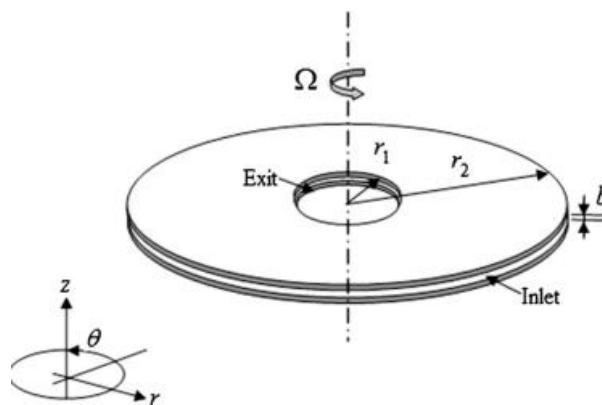


Fig. 6. The schematic diagram for the mathematic solution [35]

2.3.2 Mesh discretization

Element size is developed accordingly for 1 million elements of each design in Figure 7. The optimum number of elements is obtained from the mesh dependency check of the Tesla micro-turbine. The meshing is required to capture proximity and curvature for more accurate data processing.

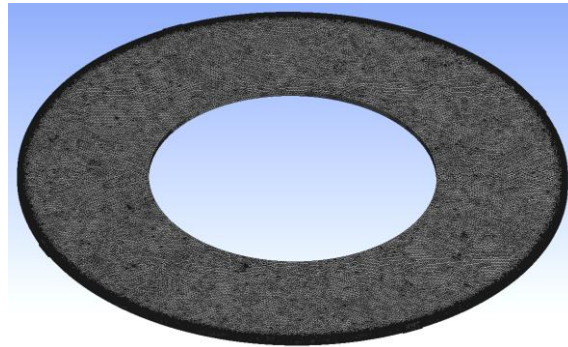


Fig. 7. Mesh element layout

Figure 8 shows the mesh dependency graph of average velocity versus the number of elements. The average velocity of 9 ms^{-1} is estimated at around 1 million elements. Hence, 1 million mesh is chosen as the optimum number of elements to be used throughout the research work.

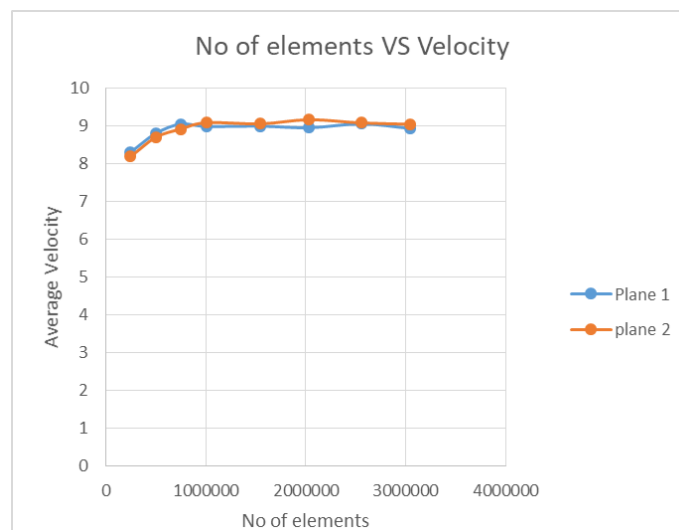


Fig. 8. Mesh dependency check of average velocity versus number of elements

2.4 Boundary Condition

Boundary condition consists of flow inlet and out boundary, wall motion and casing. A detailed view is shown in Figure 9.

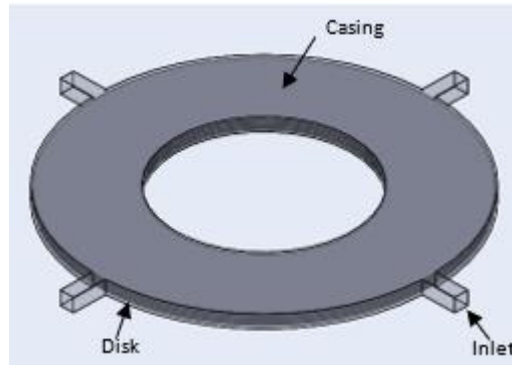


Fig. 9. Circumferential inlet

In this study, the fluid is assumed to be steady-state, incompressible and laminar flow. Referring to Table 3, the mass flow inlet with a flow rate of $30e^{-5}$ kg/s and pressure outlet with 0 Pa are used in this simulation. The casing is selected as a stationary wall with the no-slip shear condition. While, the domain disk is selected as a moving wall with a rotational speed of 800 rad/s. The boundary conditions are set similar to the work by previous study [30], as in Table 3:

Table 3

Boundary Condition [30]

Boundary condition	Values
Mass flow rate inlet	$30 e^{-5}$ kg/s
Pressure outlet	0 Pascal
Fluid type	Air, Ideal gas
Casing	Stationary wall with no slip shear condition
Domain	Moving wall with a rotational speed of 800 rad/s
Viscous model	Laminar
Residual error	10^{-6}

3. Results and Discussions

3.1 Validation of 4-Inlets and 1-Gap Turbine

This section discusses the results obtained from the validation study. The results of validation will be discussed from qualitative and quantitative perspectives in the following sub-sections.

3.1.1 Qualitative results

The qualitative analysis between the current study and the study by Sengupta [30] presented the results of pressure, radial and tangential velocities, as in Figure 10.

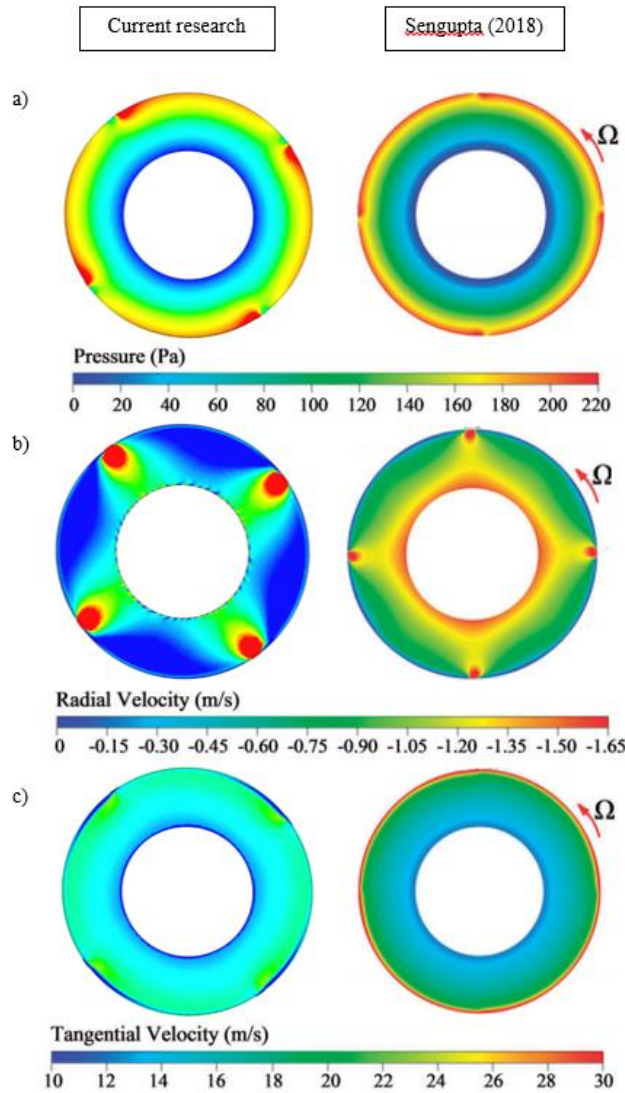


Fig. 10. Pressure, Radial and Tangential velocity contours of a single plane

For pressure contours, the pattern obtained is almost similar, with the highest pressure at the inlet and it decreasing towards the outlet. Meanwhile, the radial velocity showed similar minimum and maximum velocities obtained in both respective outlets and inlets. The negative value described that the flow is exiting towards the outlet from the outer edge of the discs. However, the distribution pattern of radial velocity showed a slight difference between both current research and the manuscript by Sengupta [30]. Besides that, the tangential velocity distribution showed a similar pattern for both comparisons with the highest at the inlet and the lowest at the outlet.

3.1.2 Quantitative results

The results have also explained the comparison between the current study and the study by Sengupta [30] from a quantitative perspective. Figure 11 shows the relationship between disc thickness to gap ratio and radial velocity for three rotational speeds of 1000 rad/s, 1500 rad/s and 2000 rad/s.

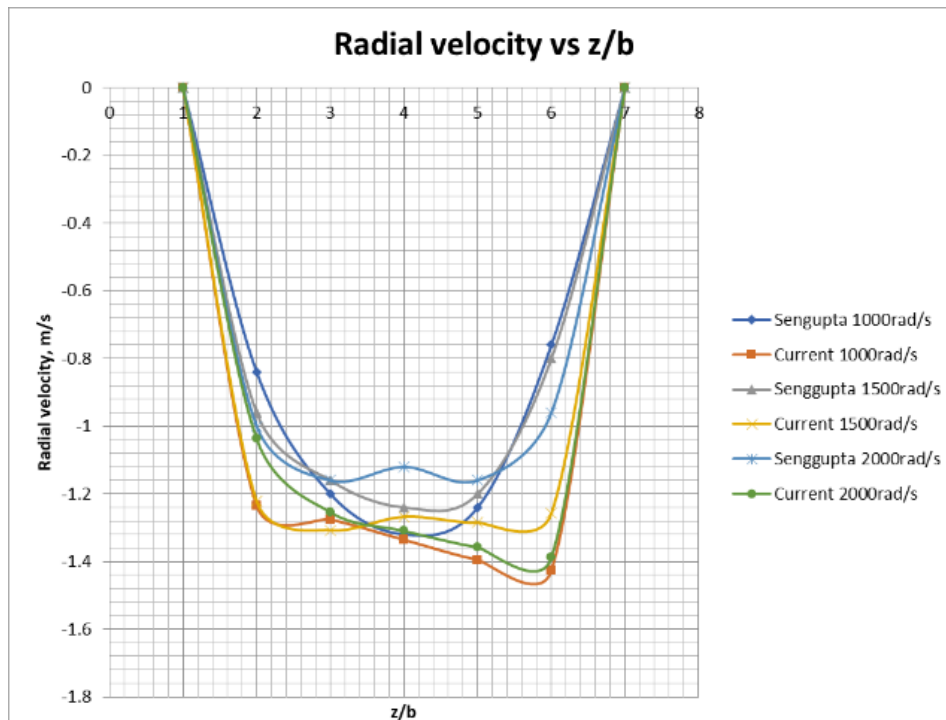


Fig. 11. Radial velocity of the current study and the study by Sengupta [30]

From Figure 11, it can be observed that the radial velocity showed high magnitude at the gap ratio $z/b = 1$ and decreased the magnitude at the middle of the gap ratio, $z/b = 4$ and finally increased the radial velocity value toward the gap ratio, $z/b = 7$. Moreover, the pattern of radial velocity at different gap ratios (z/b) showed a similar pattern at the beginning of the gap ratio and slightly different at the centre location comparing current research and the study by Sengupta [30] for 1000 rad/s, 1500 rad/s and 2000 rad/s, respectively. It can be observed that the magnitude difference between current research and validated radial velocity showed the increment as the speed of rotation increased particularly at the same z/b ratio. The average percentage error of 1000 rad/s, 1500 rad/s and 2000 rad/s were stated to be 24.40%, 18.27% and 17.55%, respectively. Mahjoob and Mani [36] clearly stated that the maximum error of CFD is 25%. Hence, this validation study is acceptable prior to further study on the analysis of the Tesla turbine. Then, for the subsequent analysis, the study can be further to understand the effect of pitot-tube to further optimize the performance of the turbine.

3.2 Study on the Effect of 'Pitot-Tube'

This section discusses the results obtained from the study on the effect of pitot-tube. The results of introducing the 'Pitot-tube' concept at the inlet represent the different number of openings, namely as 4-inlets-with-4-openings (4i4o) and 4-inlets-with-1-openings (4i1o). The comparison results between the 4i1o and 4i4o will be discussed in terms of pressure distribution, velocity distribution, torque, thrust, power and efficiency in the following sub-sections.

3.2.1 Different number of openings: pressure distribution

The results of pressure contour and pressure magnitude of 4i1o and 4i4o are presented in Figures 12 and 13.

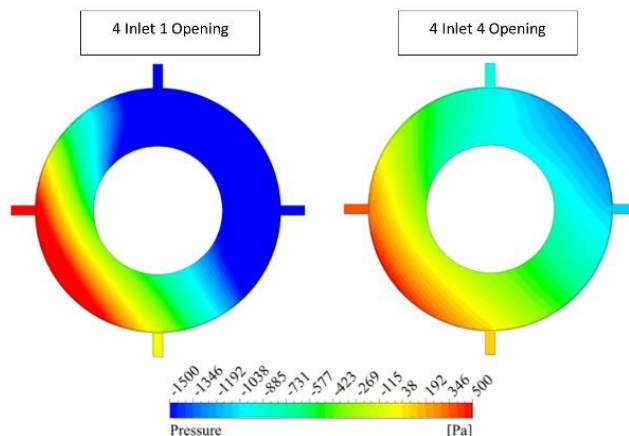


Fig. 12. Pressure contour of 4i1o and 4i4o

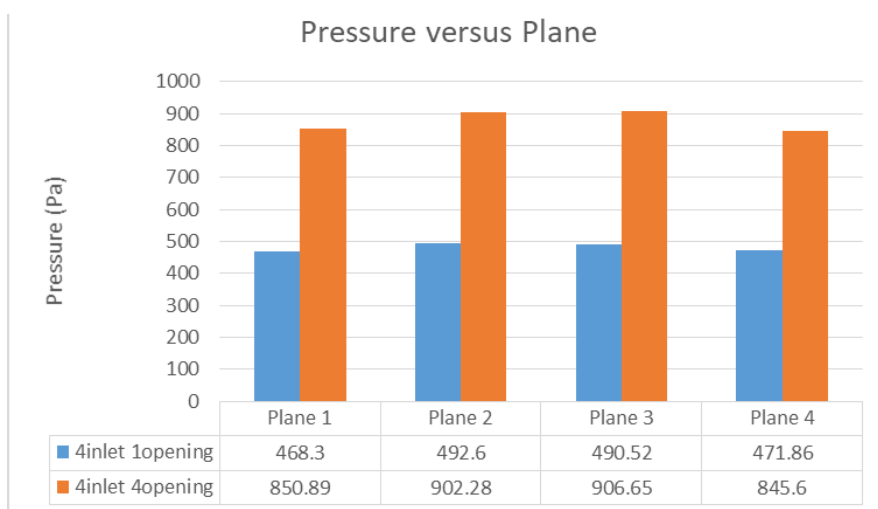


Fig. 13. Pressure magnitude of 4i1o and 4i4o at different plane sections

Figure 12 shows that the pressure contour of 4i4o has a better pressure distribution than that of 4i1o in which the high-pressure intensity occurred on the left side of the section plane and the low pressure on the right side of the section plane. The pressure magnitude of 4i4o was approximately twice as that of 4i1o for each plane section. For plane section 1, the pressure magnitude for 4i4o is reported to be 850.89 Pa, compared to 4i1o at 468.30 Pa. The pressure value increased in the middle of the disk domain, especially in plane sections 2 and plane 3, as shown in Figure 13. The pressure magnitude of 4i1o is reported as 492.60 Pa and 490.52 Pa for planes 2 and 3, respectively. Meanwhile, for 4i4o, the pressure magnitude for planes 2 and 3 is calculated as 902.28 Pa and 906.65 Pa, respectively. For plane 4, the pressure magnitude of 4i4o is calculated to be 845.6 Pa, which is 79.21% higher than the pressure magnitude of 4i1o.

From the qualitative and quantitative results of pressure distribution, the 4i4o produced higher pressure distribution than the 4i1o. The pressure distribution showed that 4i4o has a small distribution range between the lowest and highest pressure values compared to 4i1o. It has been proven that the introduction of 4-openings of the inlet nozzle has better and equal pressure distribution at each disk gap which produced better performance than 1-opening of the inlet nozzle. This is because the individual inlet produced better fluid flow distribution in between each disk gap and led to a better effect of pressure distribution.

3.2.2 Different number of openings: velocity distribution

The results of velocity value and velocity contour of radial, axial, circumferential and magnitude for respective 4i1o and 4i4o are presented in Figures 14 and 15.

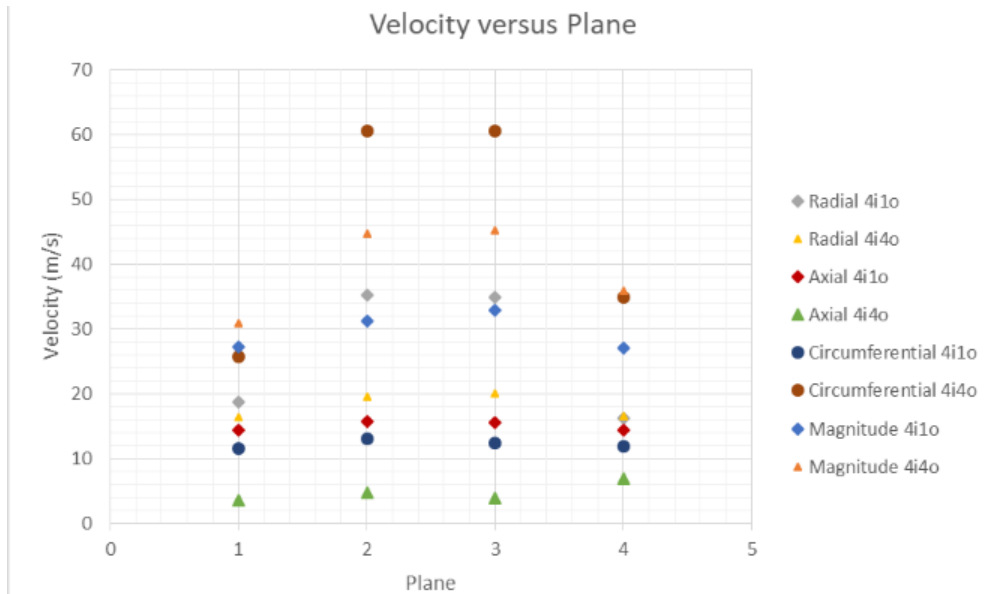


Fig. 14. Velocity magnitude of tangential, radial and axial velocity of 4i1o and 4i4o

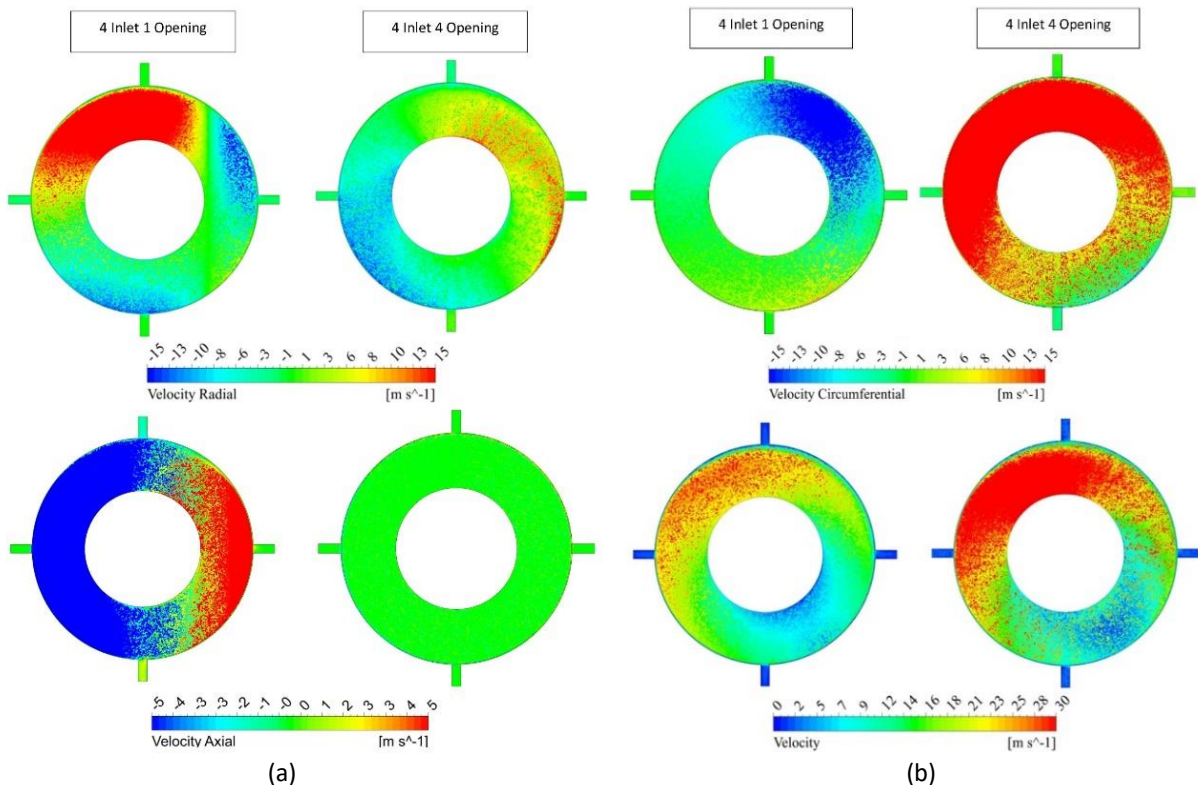


Fig. 15. (a) radial and axial velocity contour (b) circumferential and magnitude velocity contour of 4i1o and 4i4o

In Figure 14, for the radial velocity, the maximum value of 4i1o is stated to be a higher value than 4i4o for both planes 1 to 4 and reached its peak at plane 2 with 35.20 m/s and 19.59 m/s for 4i1o and

4i4o, respectively. However, the distribution of radial velocity for 4i4o showed a more equal distribution along the disk compared to 4i1o, as in Figure 15(a). A similar pattern is observed for the axial velocity distribution, with 4i4o giving a more uniform distribution along the disk compared to 4i1o. The maximum axial velocity value of plane 2 also had the highest value of 15.72 m/s and 4.79 m/s for 4i1o and 4i4o, respectively.

For the circumferential velocity in Figure 14, the 4i4o had a higher maximum value compared to the 4i1o. Plane 2 showed the highest value of 60.53 m/s and 12.99 m/s 4i4o and 4i1o, respectively. On the other hand, qualitatively, the distribution of 4i4o had a high-intensity value with one-third of the disk compared to 4i1o, in which a lower intensity value of circumferential velocity is presented along the disk surface, as in Figure 15(b).

For the magnitude velocity, it is observed that the velocity distribution of 4i4o produced a higher velocity contour on the left side of the disk than that of 4i1o, as shown in Figure 15(b). Meanwhile, the quantitative data in Figure 14 showed that the maximum magnitude velocity for 4i4o gives a higher value than 4i1o at each plane. The maximum magnitude velocity for 4i1o is stated to be 27.18 m/s, 31.31 m/s, 32.97 m/s and 27.06 m/s for planes 1,2,3 and 4, respectively. On the other hand, for 4i4o, the maximum magnitude velocity is stated to be 30.81 m/s, 44.79 m/s, 45.22 m/s and 35.86 m/s for planes 1,2,3 and 4, respectively.

Furthermore, Figure 16 showed the cross-section view of 4i1o and 4i4o.

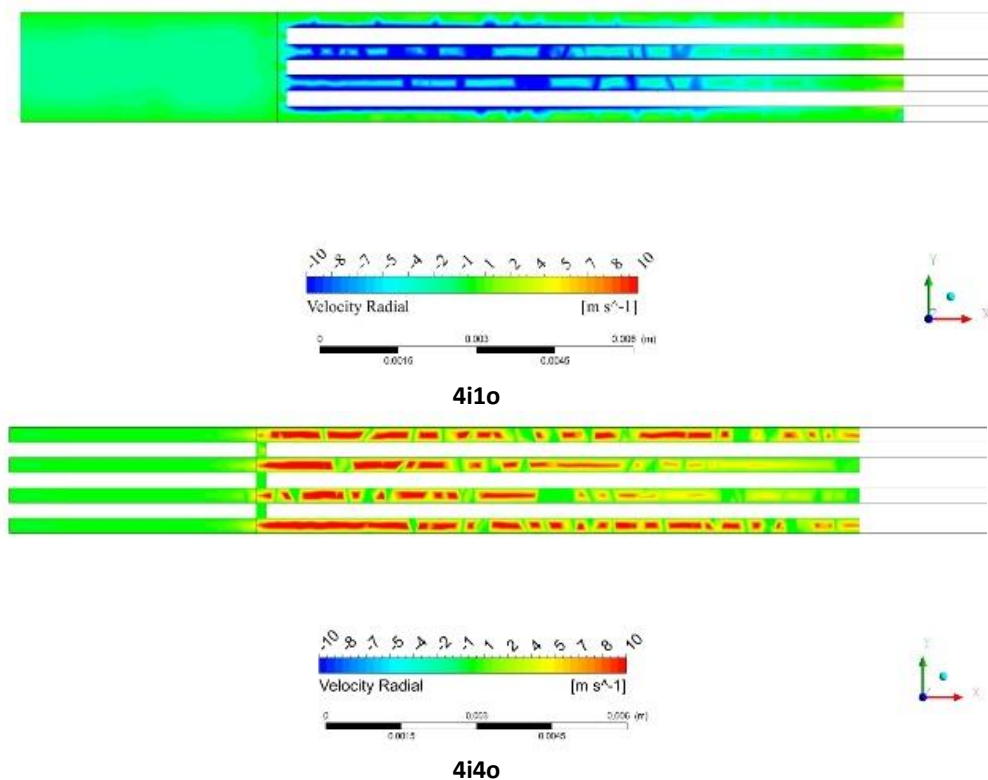


Fig. 16. Cross-sectional view of velocity for 4i1o and 4i4o

According to the quantitative and qualitative data of velocity distributions, it is proved that the existence of the individual inlet nozzle (4-openings) presented a uniform flow distribution at each disk gap compared to the 1-opening inlet nozzle. Due to this matter, the flow distribution for 4-openings produced less disturbance and recirculation flow compared to 1-opening. This circumstance is demonstrated by the increased effect of adhesion and cohesion between each disk and fluid flow particle that lead to higher energy transferred from the fluid to the shaft. Hence, a higher spinning

speed is produced and leads to higher turbine performance. Moreover, the individual opening reduced the energy losses and dissipation compared to the 1-opening inlet nozzle.

3.2.3 Different number of openings: torque, thrust, power output, and efficiency

The results of torque, thrust, power output and efficiency for both respective designs of 4i1o and 4i4o, as shown in Table 4.

Table 4

Torque, Thrust, Power Output and Efficiency of 4i1o and 4i4o

Inlet type	Torque at domain (J)	Thrust, T (N)	Power output (W)	Efficiency, η (%)
4i1o	$2.97e^{-4}$	$1.163e^{-3}$	$2.49e^{-2}$	3.11
4i4o	$3.28e^{-3}$	$1.55e^{-3}$	$2.74e^{-1}$	34.30

Referring to Table 4, the power input for both designs is stated to be 0.8 W. The obtained torque of pitot 4i1o indicated the value of $2.970e^{-4}$ J compared to 4i4o with $3.275e^{-3}$ J, which is calculated to be 10 times different. Meanwhile, 4i4o is stated to have a higher thrust magnitude of $1.55e^{-3}$ N compared to 4i1o of $1.163e^{-3}$ N with a percentage difference of 33.69%. Hence, the higher power output obtained by the 4i4o inlet is 10 folds higher than that of 4i1o of $2.74e^{-1}$ W and $2.49e^{-2}$ W, respectively. Moreover, the efficiency of 4i4o produced a higher value with 34.30% compared to the 4i1o with 3.11%. Adding the openings on the inlet helps to produce more torque, thrust and power. The adjustment made is proven that helps in producing more power for the micro-turbine.

4. Conclusions

Based on the result obtained, these combinations of pitot 4i4o have proven to be effective in producing more torque and power of 10 times higher than the 4i1o. Hence, the thrust and efficiency values also showed 33.69% and 34.30%, respectively, which is higher for 4i4o compared to 4i1o. Moreover, the pressure and velocity distributions of 4i4o also produced higher values with more uniform distribution at each gap. This optimized the effect of cohesion and adhesion between the fluid particle and disk surface has the higher energy transferred at the shaft and reduced the energy losses and dissipation. It can be concluded that the introduction of the functional theory of 'pitot-tube', which considers the gaps individually by having a separate inlet for each of them, had performed a great impact on the performance of Tesla turbine.

Acknowledgement

The authors acknowledge that the study is financially supported by Universiti Putra Malaysia under the GP-IPM research grant (Vot Number 9675000). In addition, the authors also like to express their gratitude and sincere appreciation to Department of Aerospace Engineering, Universiti Putra Malaysia for close collaboration in this work.

References

- [1] Sidik, Nor Azwadi Che, Solihin Musa, Siti Nurul Akmal Yusof, and Erdiwansyah Erdiwansyah. "Analysis of Internal Flow in Bag Filter by Different Inlet Angle." *Journal of Advanced Research in Numerical Heat Transfer* 3, no. 1 (2020): 12-24.
- [2] Khattak, M. A., NS Mohd Ali, NH Zainal Abidin, N. S. Azhar, and M. H. Omar. "Common Type of Turbines in Power Plant: A Review." *Journal of Advanced Research in Applied Sciences and Engineering Technology* 3, no. 1 (2016): 77-100.

- [3] Niknahad, Ali. "Numerical study and comparison of turbulent parameters of simple, triangular, and circular vortex generators equipped airfoil model." *Journal of Advanced Research in Numerical Heat Transfer* 8, no. 1 (2022): 1-18.
- [4] Mondal, Mithun, Djamel Hissein Didane, Alhadj Hisseine Issaka Ali, and Bukhari Manshoor. "Wind Energy Assessment as a Source of Power Generation in Bangladesh." *Journal of Advanced Research in Applied Sciences and Engineering Technology* 26, no. 3 (2022): 16-22. <https://doi.org/10.37934/araset.26.3.1622>
- [5] Gaheen, Osama A., Mohamed A. Aziz, M. Hamza, Hoda Kashkoush, and Mohamed A. Khalifa. "Fluid and Structure Analysis of Wind Turbine Blade with Winglet." *Journal of Advanced Research in Fluid Mechanics and Thermal Sciences* 90, no. 1 (2022): 80-101. <https://doi.org/10.37934/arfmts.90.1.80101>
- [6] Aldhufairi, Mohammed, Mohd Khairul Hafiz Muda, Faizal Mustapha, Kamarul Arifin Ahmad, and Noorfaizal Yidris. "Design of Wind Nozzle for Nozzle Augmented Wind Turbine." *Journal of Advanced Research in Fluid Mechanics and Thermal Sciences* 95, no. 1 (2022): 36-43. <https://doi.org/10.37934/arfmts.95.1.3643>
- [7] Miller, Gerald E., BRADLEY D. Etter, and JEAN M. Dorsi. "A multiple disk centrifugal pump as a blood flow device." *IEEE Transactions on biomedical engineering* 37, no. 2 (1990): 157-163. <https://doi.org/10.1109/10.46255>
- [8] Borate, Hanumant P., and Nitin D. Misal. "An effect of spacing and surface finish on the performance of bladeless turbine." In *Gas Turbine India Conference*, vol. 45165, pp. 165-171. American Society of Mechanical Engineers, 2012. <https://doi.org/10.1115/GTINDIA2012-9623>
- [9] Isomura, Kousuke, Motohide Murayama, Susumu Teramoto, Kousuke Hikichi, Yuki Endo, Shinichi Togo, and Shuji Tanaka. "Experimental verification of the feasibility of a 100 W class micro-scale gas turbine at an impeller diameter of 10 mm." *Journal of micromechanics and microengineering* 16, no. 9 (2006): S254. <https://doi.org/10.1088/0960-1317/16/9/S13>
- [10] Lemma, Engida, R. T. Deam, D. Toncich, and R. Collins. "Characterisation of a small viscous flow turbine." *Experimental Thermal and Fluid Science* 33, no. 1 (2008): 96-105. <https://doi.org/10.1016/j.expthermflusci.2008.07.009>
- [11] Romanin, Vince D., Vedavalli G. Krishnan, Van P. Carey, and Michel M. Maharbiz. "Experimental and Analytical study of sub-watt scale Tesla turbine performance." In *ASME International Mechanical Engineering Congress and Exposition*, vol. 45233, pp. 1005-1014. American Society of Mechanical Engineers, 2012. <https://doi.org/10.1115/IMECE2012-89675>
- [12] Holoshitz, Noa, Clifford J. Kavinsky, and Ziyad M. Hijazi. "The Edwards SAPIEN Transcatheter heart valve for calcific aortic stenosis: a review of the valve, procedure, and current literature." *Cardiology and therapy* 1 (2012): 1-17. <https://doi.org/10.1007/s40119-012-0006-8>
- [13] Foo, S. J., W. C. Tan, and M. Shahril. "Development of tesla turbine for green energy application." In *Proceeding of National Conference in Mechanical Engineering Research and Postgraduate Studies (2nd NCMER 2010)*, pp. 671-680. 2010.
- [14] Krishnan, Vedavalli G., Vince Romanin, Van P. Carey, and Michel M. Maharbiz. "Design and scaling of microscale Tesla turbines." *Journal of Micromechanics and Microengineering* 23, no. 12 (2013): 125001. <https://doi.org/10.1088/0960-1317/23/12/125001>
- [15] Guha, Abhijit, and B. Smiley. "Experiment and analysis for an improved design of the inlet and nozzle in Tesla disc turbines." *Proceedings of the Institution of Mechanical Engineers, Part A: Journal of Power and Energy* 224, no. 2 (2010): 261-277. <https://doi.org/10.1243/09576509JPE818>
- [16] Hoya, G. P., and A. Guha. "The design of a test rig and study of the performance and efficiency of a Tesla disc turbine." (2009): 451-465. <https://doi.org/10.1243/09576509JPE664>
- [17] Armstrong, James Hal. "An investigation of the performance of a modified Tesla turbine." PhD diss., Georgia Institute of Technology, 1952.
- [18] Jermihov, Paul N., Lu Jia, Michael S. Sacks, Robert C. Gorman, Joseph H. Gorman, and Krishnan B. Chandran. "Effect of geometry on the leaflet stresses in simulated models of congenital bicuspid aortic valves." *Cardiovascular engineering and technology* 2 (2011): 48-56. <https://doi.org/10.1007/s13239-011-0035-9>
- [19] Krishnan, Vedavalli G., Zohora Iqbal, and Michel M. Maharbiz. "A micro Tesla turbine for power generation from low pressure heads and evaporation driven flows." In *2011 16th International Solid-State Sensors, Actuators and Microsystems Conference*, pp. 1851-1854. IEEE, 2011.
- [20] Peshlakai, Aaron. *Challenging the versatility of the Tesla turbine: working fluid variations and turbine performance*. Arizona State University, 2012.
- [21] Holland, Kris. "Design, construction and testing of a Tesla Turbine." PhD diss., Laurentian University of Sudbury, 2016.
- [22] Li, Ruixiong, Huanran Wang, Erren Yao, Meng Li, and Weigang Nan. "Experimental study on bladeless turbine using incompressible working medium." *Advances in Mechanical Engineering* 9, no. 1 (2017): 1-12. <https://doi.org/10.1177/1687814016686935>
- [23] Ho-Yan, Bryan P. "Tesla turbine for pico hydro applications Guelph Eng." (2011): 1-8.

- [24] Rice, Warren. "An analytical and experimental investigation of multiple-disk turbines." (1965): 29-36. <https://doi.org/10.1115/1.3678134>
- [25] Crawford, M. E., and W. Rice. "Calculated design data for the multiple-disk pump using incompressible fluid." (1974): 274-282. <https://doi.org/10.1115/1.3445806>
- [26] Jędrzejewski, Łukasz, and Piotr Lampart. "Investigations of aerodynamics of Tesla bladeless microturbines." *Journal of Theoretical and Applied Mechanics* 49 (2011): 477-499.
- [27] Lampart, Piotr, Krzysztof Kosowski, Marian Piwowarski, and Łukasz Jędrzejewski. "Design analysis of Tesla micro-turbine operating on a low-boiling medium." *Polish Maritime Research* 16, no. Special (2009): 28-33. <https://doi.org/10.2478/v10012-008-0041-5>
- [28] Choon, Tan Wee, A. A. Rahman, Foo Shy Jer, and Lim Eng Aik. "Optimization of Tesla turbine using computational fluid dynamics approach." In *2011 IEEE Symposium on Industrial Electronics and Applications*, pp. 477-480. IEEE, 2011. <https://doi.org/10.1109/ISIEA.2011.6108756>
- [29] Sengupta, Sayantan, and Abhijit Guha. "A theory of Tesla disc turbines." *Proceedings of the Institution of Mechanical Engineers, Part A: Journal of Power and Energy* 226, no. 5 (2012): 650-663. <https://doi.org/10.1177/0957650912446402>
- [30] Sengupta, S., & Guha, A. (2018). Inflow-rotor interaction in Tesla disc turbines: Effects of discrete inflows, finite disc thickness, and radial clearance on the fluid dynamics and performance of the turbine. *Proceedings of the Institution of Mechanical Engineers, Part A: Journal of Power and Energy*, 232(8), 971-991. <https://doi.org/10.1177/0957650918764156>
- [31] Hoya, G. P., and A. Guha. "The design of a test rig and study of the performance and efficiency of a Tesla disc turbine." (2009): 451-465. <https://doi.org/10.1243/09576509JPE664>
- [32] Zhao, Dan, Chenzhen Ji, C. Teo, and Shihuai Li. "Performance of small-scale bladeless electromagnetic energy harvesters driven by water or air." *Energy* 74 (2014): 99-108. <https://doi.org/10.1016/j.energy.2014.04.004>
- [33] Mandal, Arindam, and Sandeep Saha. "Performance analysis of a centimeter scale Tesla turbine for micro-air vehicles." In *2017 International conference of Electronics, Communication and Aerospace Technology (ICECA)*, vol. 1, pp. 62-67. IEEE, 2017. <https://doi.org/10.1109/ICECA.2017.8203625>
- [34] Rusin, Krzysztof, Włodzimierz Wróblewski, Sebastian Rulik, Mirosław Majkut, and Michał Strozik. "Performance Study of a Bladeless Microturbine." *Energies* 14, no. 13 (2021): 3794. <https://doi.org/10.3390/en14133794>
- [35] Sengupta, Sayantan, and Abhijit Guha. "A theory of Tesla disc turbines." *Proceedings of the Institution of Mechanical Engineers, Part A: Journal of Power and Energy* 226, no. 5 (2012): 650-663. <https://doi.org/10.1177/0957650912446402>
- [36] Mahjoob, S., and M. Mani. "The Performance of Cfd Methods in Aerodynamic Estimation of Circular and Non-Circular Bodies." In *International Conference of Computational Methods in Sciences and Engineering 2004 (ICCMSE 2004)*, pp. 332-336. CRC Press, 2019. <https://doi.org/10.1201/9780429081385-81>